Nano Energy 28 (2016) 87–96

Contents lists available at ScienceDirect

Nano Energy

journal homepage: www.elsevier.com/locate/nanoen

Nanoparticle chemically end-linking elastomer network with super-low hysteresis loss for fuel-saving automobile

Jun Liu [a], Zijian Zheng [a], Fanzhu Li [a], Weiwei Lei [a], Yangyang Gao [a], Youping Wu [a], Liqun Zhang [a,b,*], Zhong Lin Wang [c,d,**]

[a] Key Laboratory of Beijing City on Preparation and Processing of Novel Polymer Materials, Beijing University of Chemical Technology, 100029 Beijing, People's Republic of China
[b] State Key Laboratory of Organic-Inorganic Composites, Beijing University of Chemical Technology, 100029 Beijing, People's Republic of China
[c] Georgia Institute of Technology, School of Materials Science and Engineering, Atlanta, GA 30332, USA
[d] Chinese Academy of Science, Beijing Institute of Nanoenergy and Nanosystem, 100083 Beijing, People's Republic of China

ARTICLE INFO

Article history:
Received 15 March 2016
Received in revised form
1 August 2016
Accepted 1 August 2016
Available online 2 August 2016

Keywords:
End-linked
Dynamic hysteresis loss
Loss factor
Fuel consumption
Nanomaterials
Tire

ABSTRACT

Achieving energy sustainability has imposed a great challenge to improve fuel efficient vehicles. Tires, to overcome the rolling resistance, are responsible for a rather large fraction of energy consumed by vehicles, and a 10% reduction in the rolling resistance corresponds to a 2% decline in the fuel consumption, which, for instance, would save 1–2 billion gallon of fuel per year consumed by the entire passenger vehicle fleet in the United States. From the materials' perspective, the key bottleneck to lower the rolling resistance of tires lies in designing a novel kind of advanced elastomeric polymer nanocomposites tailored for tire tread, with remarkably low dynamic hysteresis loss (DHL). Here we show that, a nanoparticle chemically end-linking elastomer network, with nanoparticles (NPs) acting as netpoints to chemically connect the dual end-groups of each polymer chain to form a network, exhibits excellent static and dynamic mechanical properties of super-low DHL. The DHL is reduced for ~50% compared to silica NPs filled elastomer that is conventionally used for tire tread. By taking advantage of a library of other nanomaterials such as functionalized carbon nanotube and graphene, our approach provides a versatile framework to fabricate the fuel-saving tires, opening up valuable opportunities for large-scale industrial applications of these nanomaterials in the tire industry.

1. Introduction

Tailoring the mechanical, physical and functional properties of polymeric materials by incorporating nanoparticles(NPs) has attracted a great scientific interest. For instance, tunable and enhanced mechanical properties are obtained by manipulating the self-assembly of polymer-grafted spherical NPs into various anisotropic superstructures in the corresponding homopolymer matrix [1]. The glass transition temperature T_g, closely related to the mechanical properties and thermal stability of polymers, can be shifted for over 10° with adding less than 1.0 wt% of functionalized graphene sheets [2] or polymer-grafted spherical NPs [3]. Besides the tailored properties of PNCs above, to tune the viscoelastic property of polymers by introducing NPs is of potential technological and engineering applications. Koratkar et al. [4] have shown that the epoxy thin film containing dense packing of multi-walled CNTs exhibits strong viscoelastic behavior with the loss factor being increased up to 1400% than that of the baseline epoxy, attributed to the nanotube-nanotube frictional sliding. Later on, they found that facilitating the nanotube-polymer interfacial frictional sliding can result in the equivalent damping property, with the needs to only introduce 1%–2% weight fraction of oxidized CNTs [5]. These viscoelastic PNCs can find potential applications as room- or high-temperature damping materials for reducing vibrational and acoustic effects in dynamic systems. These studies are, however, aiming at increasing the energy dissipation, and little attention has been directed to decrease the energy dissipation of PNCs, which is of paramount significance to develop fuel-saving automobile tires.

The tires are mainly composed of elastomeric nanocomposites (ENCs), by introducing the nano-sized carbon black or silica to

* Corresponding author at: Key Laboratory of Beijing City on Preparation and Processing of Novel Polymer Materials, Beijing University of Chemical Technology, 100029 Beijing, People's Republic of China.
** Corresponding author at: Georgia Institute of Technology, School of Materials Science and Engineering, Atlanta, GA 30332, USA.
E-mail addresses: zhanglq@mail.buct.edu.cn (L. Zhang), zhong.wang@mse.gatech.edu (Z.L. Wang).

http://dx.doi.org/10.1016/j.nanoen.2016.08.002
2211-2855/

remarkably improve the mechanical properties, successfully realizing the large-scale industrial application of tires. However, a homogeneous and uniform distribution of NPs in the elastomeric matrix is always difficult to achieve [6–8], and they easily tend to form aggregates, aggolomerates and eventually a three-dimensional NP physical network via direct contact between NPs or polymer chain bridges anchored between neighboring NPs [9,10]. Since this physical network is highly strain-dependent (also referred to the well-known Payne effect [11]), a harmful consequence is that the break-up and recovery of the network structure significantly increases the viscous part and the dynamic hysteresis loss (DHL), resulting in converting more energy into heat and greater energy loss under the dynamic loading-unloading condition [12], compared to the pure system. This energy dissipation remarkably increases the fuel consumption of automobile tires. Remarkably, the number of vehicles worldwide is expected to increase up to 2 billion by 2035 [13], and it is estimated that a 10% reduction in the DHL corresponds to a 2% decline in the fuel consumption, which, for instance, is estimated to annually save 1–2 billion gallons of fuel of the 130 billion gallons consumed by the entire passenger vehicle fleet in the United States [14]. And the fuel efficiency of tires, as an vital index, has been clearly enforced in the European Union Tire Label Regulation since 2012 [15]. Therefore, it is a pressing task to fabricate a new kind of ENCs with controllable uniform distribution of NPs, without any formation of the physical network via NPs, for developing green automobile tires with low fuel consumption.

In fact, as for the uniform and tunable distribution of nano-reinforcing units in the polymer matrix, thermoplastic elastomer (TPE) is born to have such structural characteristics, such as styrene-butadiene-styrene(SBS) tri-block copolymer [16] and polyurethanes (always referred to TPU). However, the nano-domains formed via Van der Waals interaction could be broken up not far above the room temperature, for instance, the working temperature to maintain good mechanical properties of most SBS and TPU is below 80 degree. This fact precludes the possibility for its practical usage in the situation of high-speed and heavy-loading tires. In addition, the terminal or end-groups of elastomeric polymer chains also increase the DHL attributed to their high mobility [17].

To address this challenge, we put forward a new concept: if we replace each nano-domain of TPE with a NP, and meanwhile the terminal-groups of polymer chains are chemically attached to the surfaces of the NPs to form a network, namely the NPs are interconnected through polymer chains with the same molecular weight, thus, this designed structure of ENCs is likely to have a much lower DHL, simultaneously with excellent mechanical strength as TPE. This is completely different from the physical network structure constructed via NPs of the conventionally physical mixing system between elastomer and NPs.

To demonstrate our concept, herein, we combine experiment and simulation, our aim is to present the first study about the DHL of this kind of ENCs, by simulating the tension-recovery deformation following our previous work [18], and experimentally measuring the storage modulus and loss factor as a function of the strain.

2. Simulation and experiment section

2.1. Simulation

To perform the simulation work, we used the classical coarse-grained molecular dynamics simulation (CGMDS), following the typical bead-spring model of polymer developed by Kremer and Grest [19]. We simulate the tension-recovery process of the ABA tri-block copolymer and the end-linked elastomer network with the NPs acting as netpoints. For the former, to obtain the spherical domains in the rubbery matrix, we directly reproduce the simulation approach from Aoyagi et al. [20]. The modeled tri-block chain length is $A_5B_{73}A_5$, and the number of polymer chains is set to be 347. We use the Lennard-Jones(LJ) potential to model the interactions between A-A blocks, B-B blocks and A-B blocks, as shown below:

$$U(r) = \begin{cases} 4\varepsilon\left[\left(\frac{\sigma}{r}\right)^{12} - \left(\frac{\sigma}{r}\right)^{6}\right] + C_1 & r < r_{cutoff} \\ 0 & r \geq r_{cutoff} \end{cases} \quad (1)$$

where C_1 is a constant which guarantees that the potential energy is continuous at the cutoff distance. Note that we use the LJ units where ε and σ are set to unit. This means that all calculated quantities are dimensionless. The interaction between the adjacent bonded beads is modeled by a stiff finite extensible nonlinear elastic (FENE) potential:

$$U_{FENE} = -0.5kR_0^2 ln\left[1 - \left(\frac{r}{R_0}\right)^2\right] \quad (2)$$

where $k = 30\frac{\varepsilon}{\sigma^2}$ and $R_0 = 1.5\sigma$, guaranteeing a certain stiffness of the bonds while avoiding high-frequency modes and chain crossing. We set different interaction strength and cutoff distance to satisfy the following two points: (1)the spherical domain of the A blocks is formed in the equilibrium state, (2) the block A, corresponding to the hard block such as the styrene blocks, behave as a glassy state, while the B blocks, corresponding to the soft bock such as the butadiene blocks, exhibit a rubbery state. Table 1a (Supplementary Note 2) shows the list of the parameters used in the interaction potential [20].

For the latter (the end-linked elastomer network with the NPs acting as netpoints), for consistency, we still use the Lennard-Jones (LJ) potential to simulate the interaction between polymer-polymer, polymer-NPs and NPs-NPs, and the FENE potential to model the bonded interaction. To account for the size effect of NPs, with its diameter equal to 4σ (the diameter of the polymer bead is σ), we use the modified Lennard-Jones function by offsetting the interaction range by R_{EV} as follows [21]:

$$U_{np}(r) = \begin{cases} 4\varepsilon\left[\left(\frac{\sigma}{r - R_{EV}}\right)^{12} - \left(\frac{\sigma}{r - R_{EV}}\right)^{6}\right] + C_2 & r < R_{EV} + r_{cutoff} \\ 0 & r \geq R_{EV} + r_{cutoff} \end{cases} \quad (3)$$

where R_{EV} is set to be 1.5σ and 3.0σ for the polymer-NPs and NPs-NPs interaction, respectively. And C_2 is a constant to satisfy that the potential energy is continuous at the cutoff distance. For better comparison, we consider and compare three systems: the pure system(system I), the direct blending between polymer and NPs (system II) and the end-linked system(system III). The parameters of the interaction potential are displayed in Table 1b (Supplementary Note 2). For system II, we set a purely repulsive interaction between NPs and NPs to achieve a dispersion state as good as possible, and we consider two cases of system II with different physical interaction strength between polymer-NPs: system II-1 (5.0), system II-2(10.0). For system III, the end-beads of polymer chains are chemically bonded to the surface of NPs through the FENE potential.

In our simulation, during equilibration the NVT ensemble is adopted to make sure that the number density of the system is set to be 0.85. We set the simulated temperature equal to $T^* = 0.4$, which is above the glass transition temperature of the rubbery B-blocks [22] and below that of the glassy A-blocks, by using the Nose-Hoover thermostat [23]. Periodic boundary conditions are

employed in all three directions during the simulation. The velocity-Verlet algorithm is used to integrate the equations of motion, with a timestep $\delta t = 0.012$, where the time is reduced by LJ time (τ).

To carry out the tension-recovery deformation, since the elastomer network is typically incompressible with its Poisson's ratio $\mu \approx 0.5$ [24], it means that its volume almost does not change when being deformed. We perform the uniaxial deformation by stretching the sample in one direction, while the other two directions will simultaneously adjust to keep the volume constant. We set the tensile and recovery strain rate $\dot{\varepsilon} = 0.026975\sigma/\tau$ in the z direction, which is the same as the simulation work from Aoyagi et al. [20]. The average stress σ in the tensile direction is obtained from the deviatoric part of the stress tensor $\sigma = (1+\mu)(-P_{zz}+P) \cong 3(-P_{zz}+P)/2$, where $P = \sum_i P_{ii}/3$ is the hydrostatic pressure, which is followed from Curro et al. [25]. All MD runs are carried out through the large scale atomic/molecular massively parallel simulator (LAMMPS), which is developed by Sandia National Laboratories [26]. More detailed simulation techniques can be found in our recent work [18].

2.2. Experiment

2.2.1. Thermoplastic styrene-butadiene-styrene (SBS) elastomer

Film casting method: We dissolved SBS in the cyclohexane, with the weight fraction equal to 15%. We got this solution with 200 ml to be mixed with pure water with 200 g. Then we gradually volatilized the solvents in the environment of cyclohexane. The obtained thin film was then dried in the vacuum. For good phase-separated morphology, we immersed this thin film in the cyclohexane for 8 h, and then was dried again in the vacuum, followed by the dynamic mechanical measurements.

2.2.2. Thermoplastic polyurethanes (TPU) elastomer

TPU elastomer with the hard segments content of 16.8% is synthesized through a two-step reaction. In the first step, a Poly (carbonate urethane) (PCU) pre-polymer(NCO%=3.6%) is prepared by the reaction of 1,4-phenylene diisocyanate(PPDI) with poly (carbonate diol) (PCDL) at 60–80 °C for 2–2.5 h. In the second step, 1,4-butanediol (BDO) as chain extender and trimethylolpropane (TMP) as cross-linking agent are added into the PCU pre-polymer and mixed for 3–4 min at 60–80 °C. The mass ratio of BDO to TMP is 1: 4 and the molar ratio of NCO groups to OH groups is 1.05: 1. The resulting compound is then casted into a sheet-mold and cured at 100 °C for 24 h. The cured samples are stored for at least one week before tests. The information of above chemicals are as follows: PCDL, M_n=200 g/mol, purchased from Nippon Polyurethane Industry Co., Ltd., Japan; PPDI, purchased from Kaixin Reagent, China, BDO with the purity of 99%, purchased from Alfa Aesar and trimethylolpropane, purity of 99%, purchased from Adamas.

2.2.3. end-linked Polydimethylsiloxane (PDMS) network

(a) The surface functionalization of silica NPs: The 1.5 g Ludox-SM30 colloidal silica (30 wt%, Sigma Aldrich) is diluted with 11 ml deionized water in the flask. At the same time, the (2 g) 3-(trihydroxysilyl)–1-propane sulfonic acid (SIT, 40 wt%,J&K Scientific Ltd) is diluted with 10 ml deionized water. The silica diluents is slowly added to the SIT diluents, while stirring vigorously with the 400 rpm speed of the paddle. And then for the mixture, a solution of sodiumhydroxide(1 mol/l) is added dropwise slowly until the pH of the solution is about 5.The entire solution is then heated by water-bathing at 70 °C and stirred vigorously for 24 h. At last, the product solution is poured into the beaker and the solvent is removed by slow heating at 60 °C.

(b) Silica NPs grafted with PDMS chains with amine end-groups: the resulting sulfonic acid functionalized particles from the first step (0.1 g) is added into 30 ml chloroform in erlenmeyer flask while stirring vigorously and then 5 g Diamino-functionalized PDMS (Sigma Aldrich) are added slowly. The mixture is required to react for about four days at the room temperature while stirring. The amine end of the PDMS react with the sulfonic acid groups on the particles, and at last, the product contains PDMS-grafted silica with free amine groups at the chain end.

(c) The excess hexamethylenediisocyanate (HDI, Sigma Aldrich) is added into the solution from the second step for cross-linking the end amine group of PDMS, then stirring six hours. The product solution is poured into the Teflon molds, and the solvent is evaporated at 70 °C for about 60 h.

To characterize the micro-phase separated structure of SBS and end-linked PDMS, we use transmission electron microscopy (TEM) carried out with an acceleration voltage of 200 kv, and we use $OsO_4$to dye the double bonds located in the soft butadiene segment, making the butadiene blocks darker than the styrene blocks, while for PDMS, we do not use OsO_4. Because of the difficulty in dying TPU via OsO_4, atomic force microscopy (AFM), which is a new type of peak force tapping AFM (PF-AFM) (NanoscopeIIIa, Brukercorporation, Germany) because of its higher resolution, is used to characterize the TPU sample. Before characterization, the samples are polished at −130 °C by using a cryo-ultramicrotome (Leica EM UC7; Germany).

To measure the dynamic mechanical properties, we adopt the commonly used Rubber Processing Analyzer (RPA2000, Alpha Technological) to obtain the storage modulus G' and loss factor tan δ as a function of the strain amplitude, by measuring at the temperature of T=60 °C and frequency F = 10 Hz, and the strain sweep is changed from 0.28% to 400%. For the end-linked PDMS via silica.

2.2.4. Physically mixed PDMS and silica

We mix the polydimethylsiloxane (PDMS) elastomer matrix with 70phr(parts per hundred parts of rubber) precipitated silica, and 2,5-Dimethyl-2 ,5-di (*tert*-butylperoxy) hexane and hydroxy silicone oil are introduced to cross-link and improve the processing property. The dynamic mechanical properties are as well carried out by varying the strain from 0 to 20% at the temperature T=60 °C and frequency F=10 Hz.

3. Results and discussion

In light of the convenience of computer simulation compared to experiment in adjusting the physical parameters, firstly, we construct sphere-like and uniformly dispersed nano-domains through the self-assembly of ABA tri-block copolymer, as shown in Fig. 1a. In theory, the more stable the structure of the uniformly dispersed nano-domains, the smaller the dynamic hysteresis loss will be, and this stability is directly related to the interaction strength between A-A blocks. To verify this inference, we change the interaction strength between A-blocks ranging from ε_{A-A} = 1.0 to 8.0, after enough equilibration we perform the tension-recovery test, and the deformed snapshots are displayed in the case of ε_{A-A} = 5.0 in Fig. 1b. Obviously, the structure of the nano-domains is not destroyed during the tension-recovery process. The corresponding stress-strain curves for various ε_{A-A} are shown in Fig. 1c. With the increase of ε_{A-A}, its mechanical property accordingly increase. One explanation results from that the nano-domains

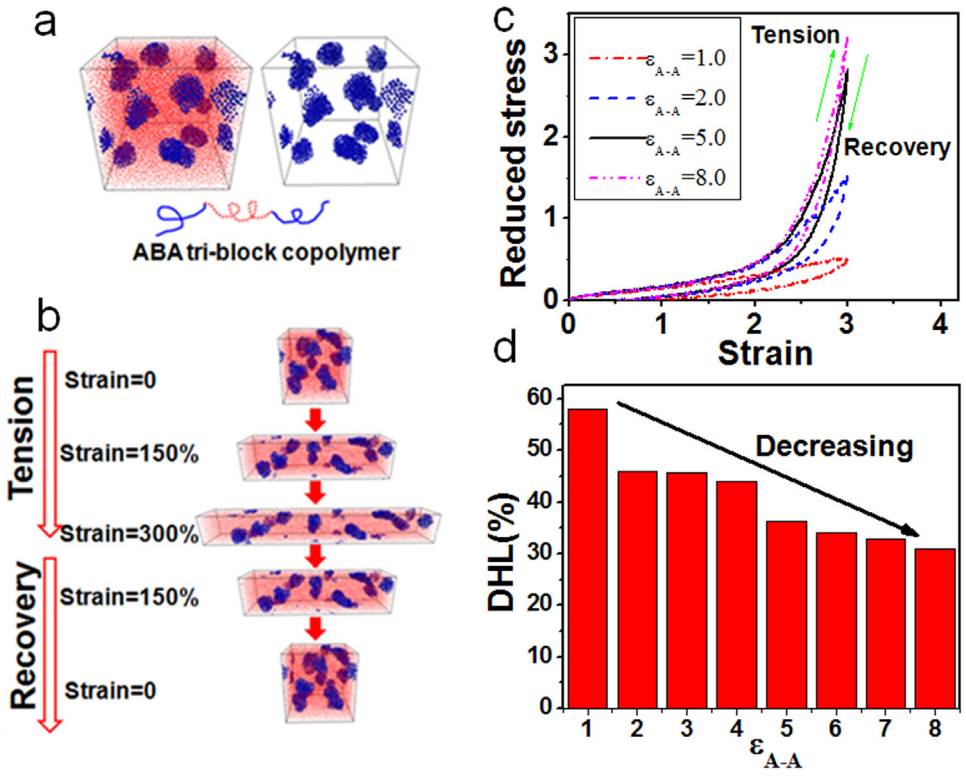

Fig. 1. Dynamic mechanical property of tri-block copolymer. (**a**) Simulated morphology of micro-phase separated structure of ABA tri-block copolymer. (**b**) Snapshots of the tension-recovery process. Effect of the interaction strength between A-A blocks (**c**) on the tension-recovery stress-strain behavior. (**d**) Dynamic hysteresis loss(DHL) derived from (**c**) for various interaction strength between A-A blocks.

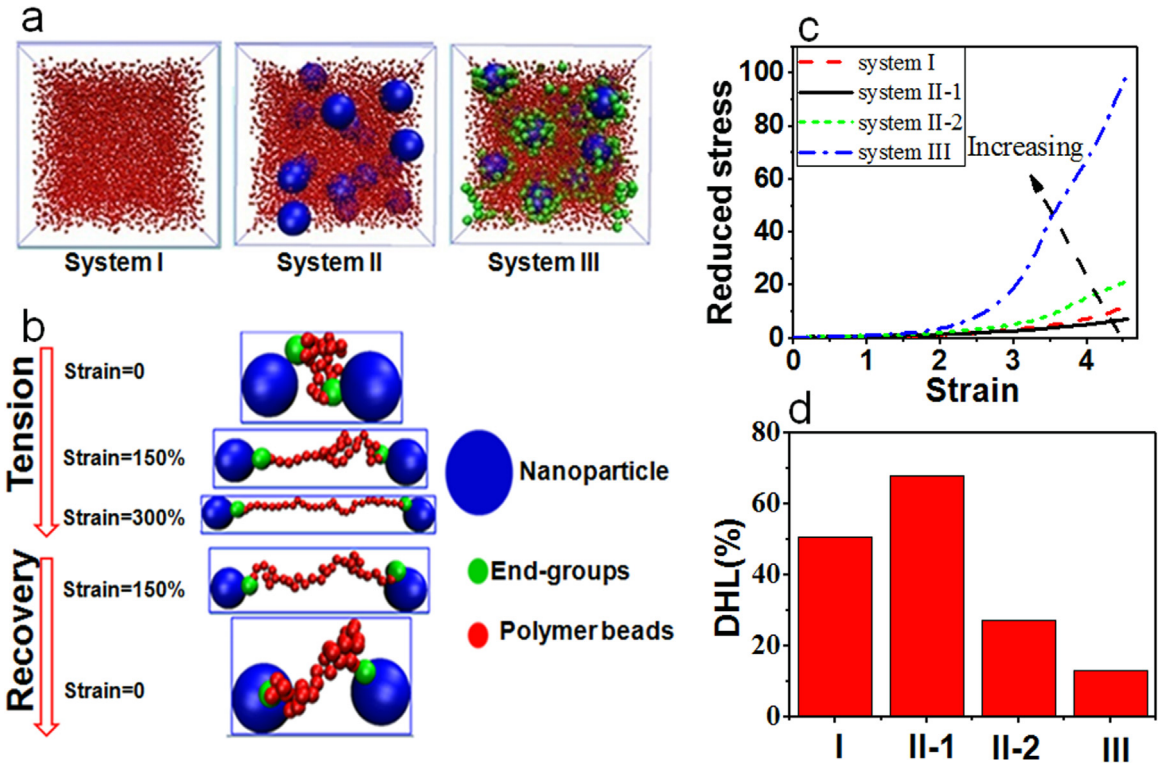

Fig. 2. Comparison of the three different elastomer nanocomposite systems through simulation. (**a**) For three systems with the same cross-linking density: system I represents pure cross-linked one, system II stands for physical interaction between spherical NPs and polymer chains, system III denotes end-linked network formed through end-beads of polymer chains chemically bonded to spherical NPs. Note that the blue spheres represent NPs, the small green beads stand for end-beads of polymer chains and the red beads denote polymer chains. (**b**) Snapshot of system III during tension-recovery process, indicating the reversible deformation of one single chain with its two ends chemically bonded to NPs. (**c**) Comparison of the stress-strain curves for system I, II and III. System II-1 and II-2 represent the attractive interaction strength between polymer and NPs equal to 5.0 and 10.0. (**d**) Comparison of the dynamic hysteresis loss(DHL) for all systems.

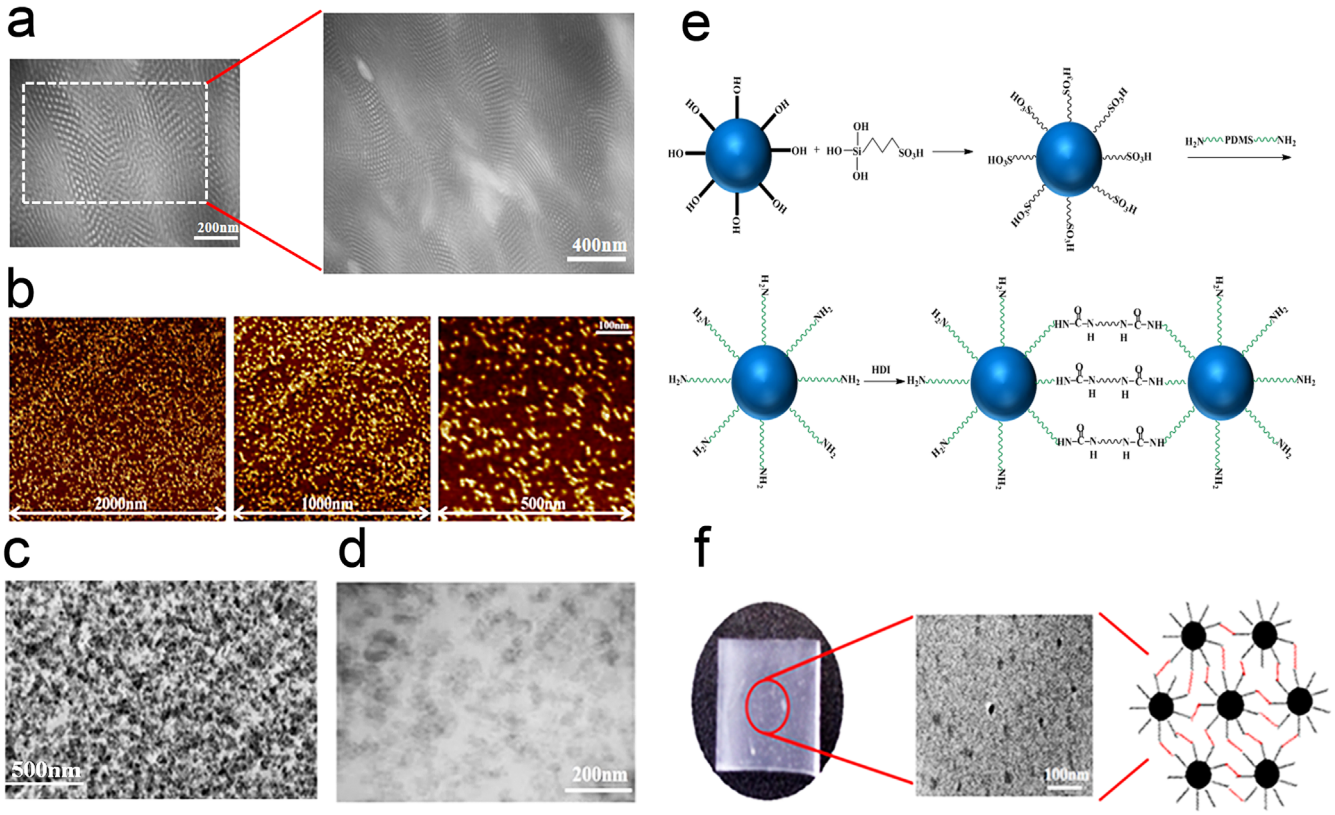

Fig. 3. Comparison of the five different elastomer nanocomposite systems through experiment. (**a**) Transmission electron microscopy of micro-phase separated structure of SBS tri-block copolymer, with the spherical hard domains formed by the styrene blocks being uniformly distributed in the butadiene blocks. (**b**) Atomic force microscopy of micro-phase separated structure of PU on different scales, with the nano-ribbon-like domains of hard segments embedded in the soft segment phase. (**c**) Transmission electron microscopy of 70 phr (per hundreds of rubber) silica nanoparticles dispersed in natural rubber (NR), by adding the coupling agent KH590 with 7phr. (**d**) Transmission electron microscopy of 65 phr carbon black(N330) dispersed in NR. (**e**) Synthesis route to prepare the end-linked PDMS network by employing silica NPs as netpoints. (**f**) The structure of the end-linked PDMS on different length scales.

formed by A-blocks become more stable, and much higher orientation of polymer chains of B-blocks under tension occur (Supplementary Fig. S1). The rubbery polymer chains of B-blocks still maintain some orientation for all ε_{A-A}, as indicated by the non-zero value of $<P_2(cos\theta)>_{B-blocks}$ when the stress becomes zero during the recovery process, which, however, decreases with the increase of ε_{A-A} (Supplementary Fig. S1).The dynamic hysteresis loss (DHL) is defined to be the ratio of the dissipated energy to the stored energy during the tension-recovery process in Fig. 1c, we obtain the change of the DHL as a function of ε_{A-A} in Fig. 1d, and a gradual decrease of DHL is seen, which, therefore, supports our assumption that stronger interaction between A-A blocks lead to more stable network structure, and less DHL.

Then how to achieve a nano-structured morphology with its stability as excellent as possible? We put forward a new kind of ENCs, namely the dual functional end-groups of each polymer chain will be chemically attached to the spherical NPs, leading to the formation of a three-dimensional network with the NPs acting as netpoints. In this case, the NPs will be uniformly dispersed because any two neighboring NPs are separated by the chemically attached polymer chains. Moreover, each NP is an entirely reinforcing unit, which can not be further broken under deformation. We adopt the simulation synthesis approach to successfully prepare such an ENCs with polymer chains being chemically end-linked to NPs, denoted by system III, and its morphology is shown in Fig. 2a. The surface of each NP is coated with the end-beads of polymer chains and well dispersed. The morphologies of the pure system (system I), and direct blending between polymer and NPs (system II) are also presented in Fig. 2a. For system II, we consider two cases with different physical interaction strength between polymer-NPs: system II-1(5.0) and system II-2(10.0). We compare their stress-strain behavior in Fig. 2c, and system III exhibits the best performance. For system III, it is interesting to note that at small strain less than 200%, its stress-strain behavior exhibits no difference compared to those of other systems, but at strain greater than 2.0, the stress begins to increase sharply, attributed to the fact that the polymer strands begin to become straightened to sustain the external force. Meanwhile, in Fig. 2b we show the snapshot of one single polymer chain with its two ends being attached to two NPs during the tension-recovery process. It is observed that this polymer strand will become straightened at large strain, and return back to the coiled state during the recovery process. The snapshot shows the irreversible desorption-adsorption process during the tension-recovery process of the physical mixing system with the physical interaction strength between polymer-nanoparticles (NPs) equal to 5.0 (Supplementary Fig. S2). The orientation of polymer chains is the largest for system III (Supplementary Fig. S3). Similarly, we obtain the change of the DHL from the tension-recovery stress-strain curves in Fig. 2d. Obviously, system III has the smallest DHL around 14%, even much smaller than that of tri-block copolymer in Fig. 1d. Therefore, these results just illustrate that the ideal structure of ENCs with low DHL is that polymer chains are chemically end-linked to NPs.

Meantime, we also simulate the effect of the volume fraction of the NPs ϕ of the end-linking system such as $\phi = 3.26\%$, 4.90%, 6.53%, 9.52% and 12.4% (Supplementary Fig. S5a) , note that only one single polymer chain with its two end-groups being chemically attached to the neighboring NPs is shown in each system. With the increase of the loading of the NPs, the cross-linked bonds on each nanoparticle decreases. Correspondingly, the stress-strain

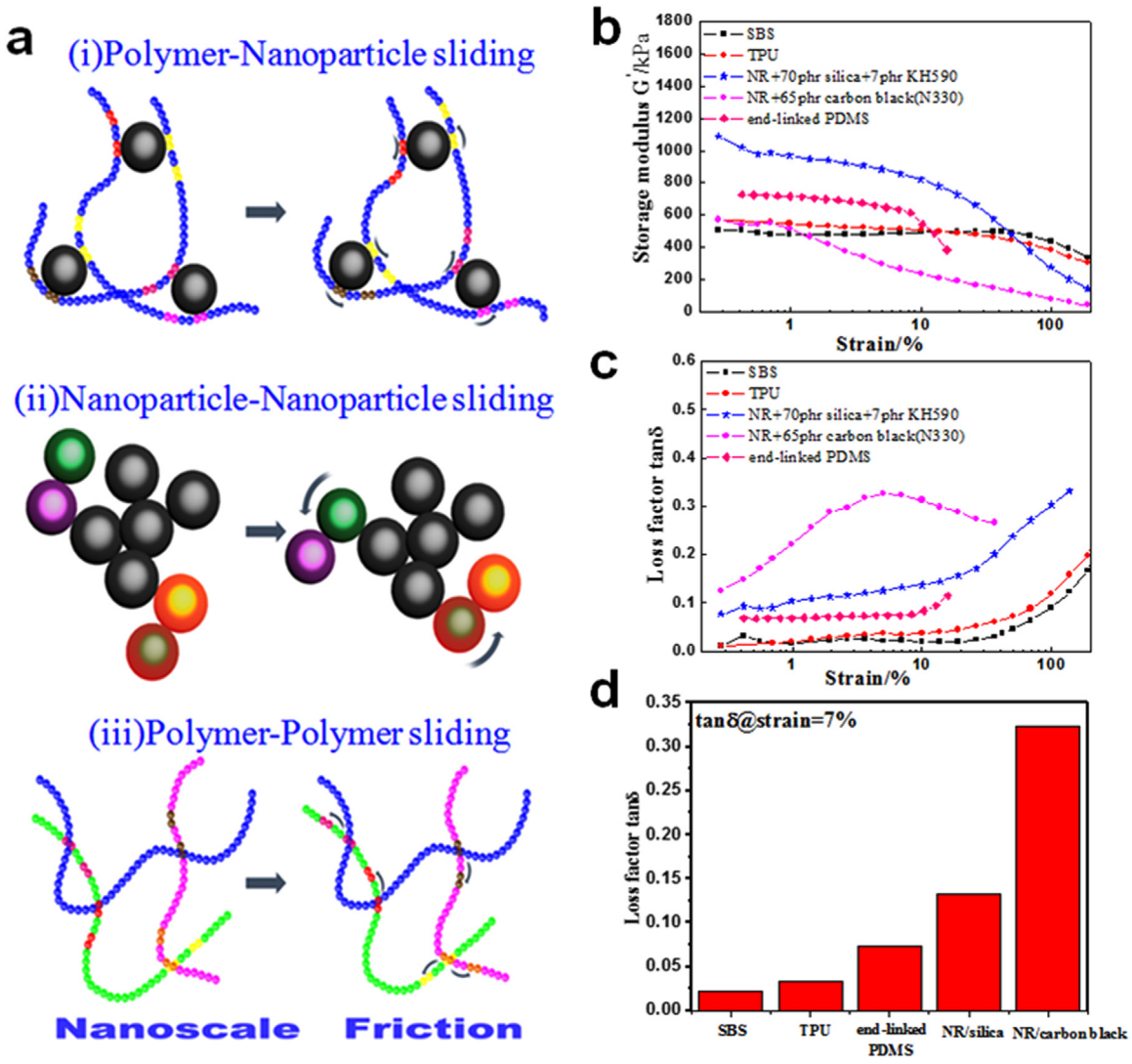

Fig. 4. Dynamic Mechanical Analysis of SBS and TPU samples as a function of the strain amplitude.**(a)**Schematics of the three typical nano-scale frictions because of the relative motions, contributing to the dynamic hysteresis loss of elastomer nanocomposites: (i)polymer chain-nanoparticle friction, (ii)nanoparticle-nanoparticle friction and (iii)polymer chain-polymer chain friction. (**b**) the storage modulus G' and (**c**) loss factor tan δ. For comparison, the natural rubber (NR) filled with 70phr silica and 7phr KH590 together with NR filled with 65phr carbon black N330 are also added. (**d**) Comparison of the value of the loss factor at the strain equal to 7% for these five systems at the temperature of 60°.

in Fig. S5(b) and the orientation of polymer chains as a function of the strain in Fig. S5(c) are both greatly decreased with ϕ. By analyzing the tension-recovery process and the stress-strain curves, we obtain the dynamic hysteresis loss(DHL) and the elastic modulus versus ϕ, as shown in Fig. S5(d) and (e). Interestingly, the smallest DHL occurs in the case of $\phi = 4.90\%$, while the elastic modulus gradually decreases. It seems that there exists a compromise between the static mechanical property and the DHL, which should be balanced when designing high performance elastomer nanocomposites.

To verify the above simulated results, we choose SBS and TPU samples, corresponding to the simulated ABA tri-block copolymer, to perform the following experimental work, and they have a stable nano-structured morphology like that of nanoparticle net-point network. For the morphology characterization of the synthesized SBS and TPU samples, the TEM result of SBS is shown in Fig. 3a. Obviously, well-defined spherical nano-domains are observed, formed by the styrene-blocks. And these domains are uniformly distributed in the whole matrix formed by the butadiene-blocks, achieved through the automatic self-assembly process because of the incompatibility between styrene and butadiene blocks. In Fig. 3b we present AFM photographs of TPU on three scales such as 2000 nm, 1000 nm and 500 nm, respectively, which are used to validate that the hard segments, indicated by the bright nano-sized domains, are distributed homogeneously in the whole matrix composed of the soft segments. This well dispersed state is as well obtained driven by the self-assembly process.

For comparison, the TEM result of 70phr(per hundreds of rubber) silica nanoparticles dispersed in natural rubber with 7phr coupling agents (KH590) and 65phr carbon black(N330) dispersed in natural rubber are displayed in Fig. 3c and d, respectively, which are commonly used as the experimental recipes for automobile tires for ensuring reinforcing effect. Obviously, silica or carbon black particles both form strong aggregation, which corresponds to the simulated system II-2 and system II-1, respectively. Meanwhile, we also synthesize a polydimethylsiloxane (PDMS) network by employing the silica NPs as netpoints, as shown in Fig. 3e, corresponding to the simulated system III. Fig. 3f confirms a uniform dispersion of silica NPs in the polymer matrix.

After checking that the synthesized SBS and TPU samples have well distributed nano-reinforcing domains, next we use the RPA

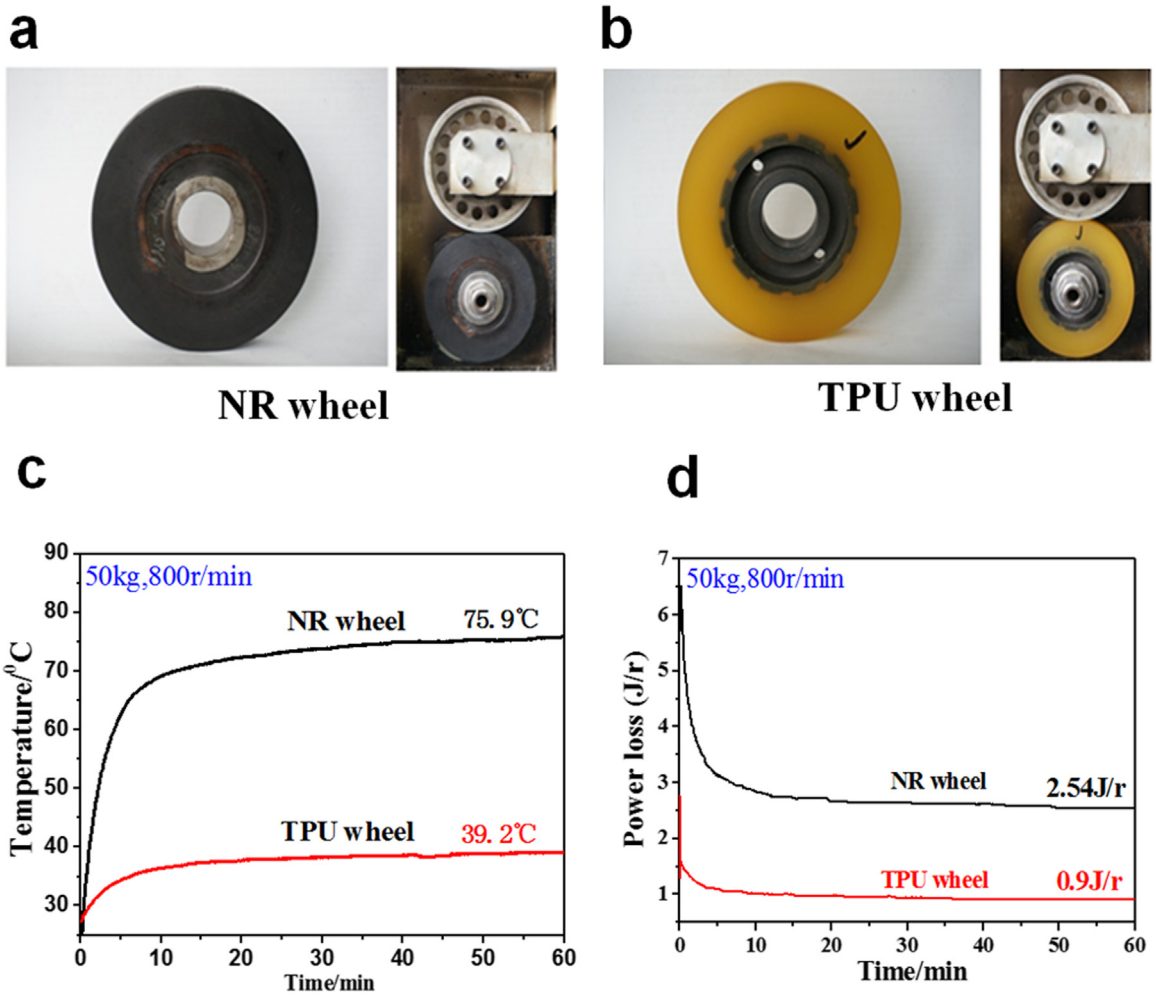

Fig. 5. The temperature increase for two wheels made of different elastomer nanocomposites. Photos of wheels made of (**a**) natural rubber(NR) filled with carbon black N330 and (**b**) thermoplastic polyurethane(TPU). The photos display the corresponding measurement condition such as loading(50 kg) and rotating velocity(800/min.). (**c**) The temperature change as a function of the time for NR and TPU wheel, with the wheel temperature becoming 75.9 °C and 39.2 °C after one hour, separately. (**d**) The power loss as a function of the time for NR and TPU wheel, with the value becoming fixed at 2.54 J/r and 0.9 J/r, separately.

apparatus to probe its dynamic mechanical property, together with that of the cases of natural rubber (NR) filled with 70phr silica NPs and 7phr KH590, natural rubber (NR) filled with 65phr carbon black(N330)and the end-linked PDMS network. It is noted that compared to carbon black, silica has worse affinity with polymeric chains, and the coupling agents are always introduced to enhance the interfacial interaction and improve the dispersion level.

Noteworthily, it is now well established that the visco-elastic nature of elastomer nanocomposites tailored for tire tread leads to the occurrence of the hysteresis loop under the loading-unloading process when tires are running on the roads, which, at the molecular level, results from the nano-scale frictions between polymer chains-polymer-chains, polymer chains-nanoparticles and nanoparticles-nanoparticles because of the relative motions, as schematically displayed in Fig. 4a. In quantitative, the relation between the energy loss and the visco-elastic property have been derived as follows: under the sinusoidal deformation, the corresponding dynamic stress and strain are given by $\sigma(t) = \sigma_a \sin \omega t$ and $\varepsilon(t) = \varepsilon_a \sin(\omega t - \delta)$, respectively. Energy loss per cycle per unit volume H under a controlled energy cycle is given as follows:

$$H = \int_0^{2\pi/\omega} \sigma(t)\frac{d\varepsilon(t)}{dt}dt = \pi\sigma_a\varepsilon_a \sin\delta \approx \pi\sigma_a\varepsilon_a \tan\delta \quad (4)$$

where σ_a is stress amplitude, ε_a is strain amplitude, ω is angular frequency, t is time, δ is phase difference between strain and stress, and $\tan\delta$ is loss factor. Evidently, the energy loss H is proportional to $\tan\delta$ at fixed deformation states.

Fig. 4b and c show the change of the dynamic storage modulus G' and loss factor $\tan\delta$ as a function of the strain. Within the range of the strain from 0.28% to 100%, both G' and $\tan\delta$ of SBS and TPU samples exhibit a long stable plateau, beyond 100% G' begins to decrease and $\tan\delta$ starts to increase, indicating the structure with nano-domains, uniformly dispersed formed through self-assembly, begin to undergo breakage, leading to the increase of the energy dissipation. However, the values of $\tan\delta$ at the strain greater than 100% for SBS and TPU are still much smaller than those of NR filled with silica or carbon black systems. For the end-linked PDMS system, we as well observe a plateau behavior of G' and $\tan\delta$ as a function of the strain. And for the NR filled with 70phr silica or 65phr carbon black, an obvious non-linear change of G' and $\tan\delta$ in the whole studied strain is observed. This is attributed to the inhomogeneous dispersion and strong aggregation of silica or carbon black NPs, which is very sensitive to the strain sweep, and will experience the broken-up even under a small strain. Hence, the automobile tires made of those ENCs, with such a non-uniform distribution state, always have high DHL and great fuel consumption. It is noted that although the added silane coupling agents can improve the dispersion, but a homogeneous and nano-scale distribution of silica NPs in the elastomer matrix is

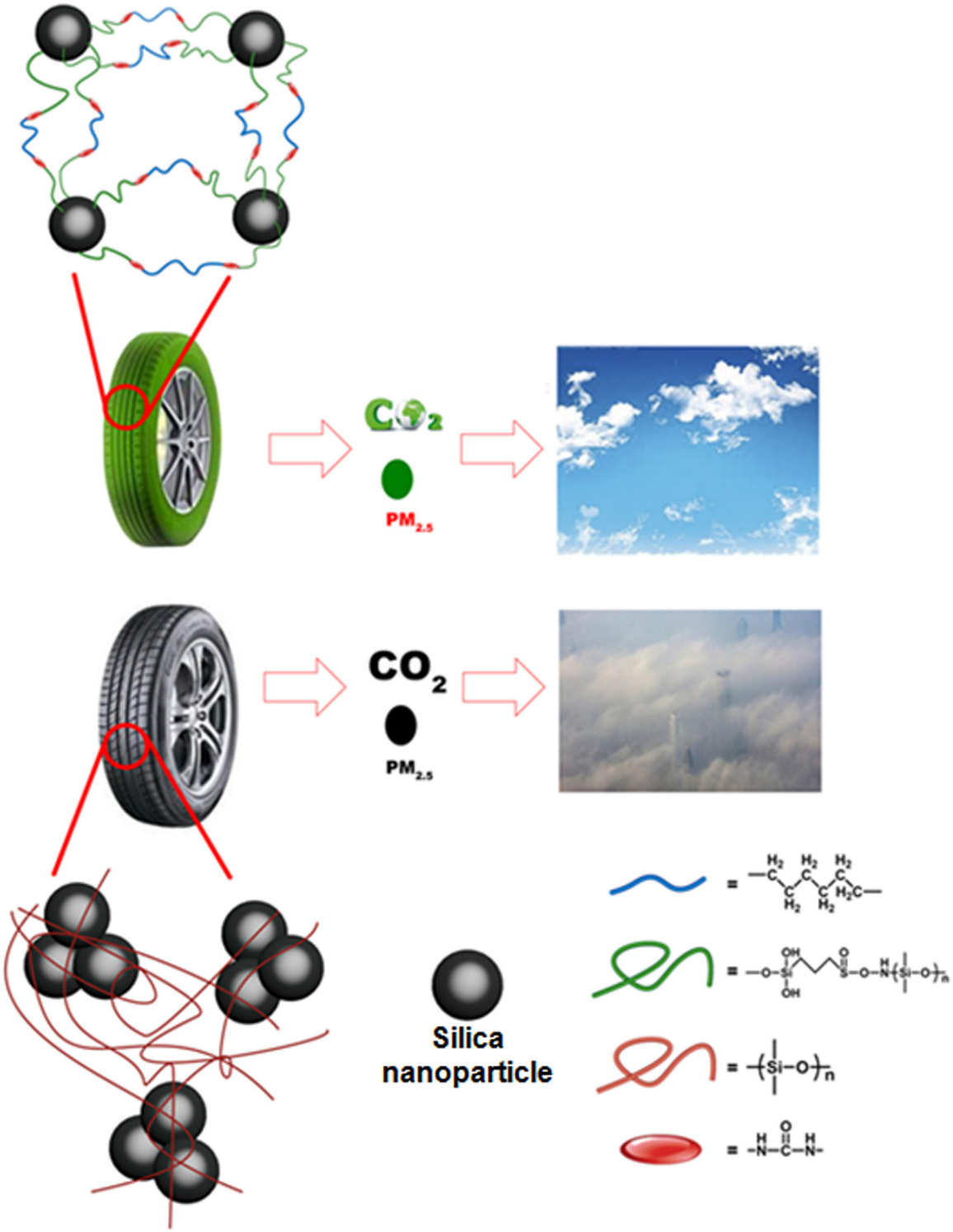

Fig. 6. Illustration of the contrast between the fuel-saving tire and the traditional one in the aspects of energy consumption and environment influence. The structure of the former is made of a nanoparticle chemical network with the homogeneous distribution of silica NPs similar to Fig. 3e, while the latter is composed of the heterogeneous distribution of NPs.

nearly impossible to achieve, particularly when the content of silica is high as much as 70phr. For further quantitative comparison, we extract the values of tan δ at the strain equal to 7% under the temperature equal to 60° and the frequency equal to 10 Hz for the five systems in Fig. 4d, which is always used as an indicator to reflect the rolling resistance of tires. The figure shows a remarkable decrease of tan δ for SBS, TPU and end-linked PDMS samples, in comparison with those of NR filled with silica or carbon black systems. For instance, around 50% of tan δ is reduced for the end-linked PDMS system, compared to that of NR/silica system.

Furthermore, by comparing the change of the storage modulus G' and the loss factor tan δ as a function of the strain between the end-linked PDMS via silica and the physically mixed PDMS-silica, we can observe that the end-linked PDMS exhibits a much weaker non-linear behavior for G' as a function of the strain, and a much smaller tan δ(Supplementary Fig. S4).

Generally, from Fig. 4 we summarize that compared to NR filled with silica or carbon black, the end-linked system exhibits much smaller loss factor, which, however, is a little larger than those of the SBS and TPU samples. We interpret this result as follows: this synthesis route in Fig. 3e involves several chemical reaction procedures, especially the grafting of the end-groups of polymer chains onto the surface of silica NPs is difficult, which directly influences the network structure and the dispersion of silica NPs. In the future for practical applications, more work about this synthesis efficiency is desirable.

Lastly, we fabricate two types of wheel, made of natural rubber filled with N330 and thermoplastic urethane(TPU), separately. It is noted that to prepare a whole tire needs a large amount of materials, and it is common to measure the wheel as a reasonable alternative. And the hard segments of the synthesized TPU is made of PPDI (*p*-Phenylenediisocyanate), which possesses the best thermal stability with the temperature up to 120°. Therefore, we choose TPU to compare with natural rubber filled with N330. One effective approach to examine the effect of the DHL is to monitor the change of the temperature during the rotating process, which is carried out by setting the loading equal to 50 kg and wheel rotating velocity equal to 800/min., as shown in Fig. 5a and b for NR wheel and TPU wheel, separately. The change of the temperature for NR and TPU wheel as a function of time during the rotating process is presented in Fig. 5c. Obviously, compared to the wheel conventionally made of natural rubber, the TPU wheel exhibits much smaller temperature increase, indicating that the TPU wheel possesses a much lower tan δ and DHL. The power loss displayed in Fig. 5d as well supports that the TPU wheel exhibits much smaller energy consumption compared to that of the NR wheel.

However, we should note that, although automobile tires made of TPU have super-low DHL and small temperature raise during rolling, the thermal stability of the reinforcing nano-domains formed through self-assembly is not good enough, especially for tires with high speed and heavy loading, which precludes its practical application as automobile tires on a large scale. Conversely, the end-linked system is more ideal and practical to be used for fuel-saving tires, and also exhibiting much reduced DHL compared to that of the present ENCs for tires.

4. Conclusions

In general, here we carry out a detailed simulation and experiment work to confirm that, nanoparticle chemically end-linking elastomer network (NCEEN), with nanoparticles (NPs) acting as netpoints to chemically connect the dual end-groups of each polymer chain to form a network, exhibits excellent static and dynamic mechanical properties, highlighting a super-low DHL. The DHL is reduced for ~50%compared to silica NPs filled elastomer that is conventionally used for tire tread. The underlying mechanism results from the stable and homogeneous distribution of NPs in the whole matrix. This NCEEN can as well be extended to carbon nanotube and graphene NPs acting as netpoints. Facing the large amount of the emission of the carbon dioxide and fine particulate matter ($PM_{2.5}$) caused by a considerable number of tires worldwide, the application of this NCEEN aimed for the next generation of tire tread will be a great contribution for energy saving and environment protection, as depicted in Fig. 6.

Acknowledgments

The authors acknowledge financial supports from the National 973 Basic Research Program of China 2015CB654700(2015CB654704), the Foundation for Innovative Research Groups of the NSF of China (51221002 and 51521062), the National Natural Science Foundation of China (51333004 and 51403015), the Major International Cooperation (51320105012) of the National Nature Science Foundation of China. The super-calculation center of "Tianhe number one" and the cloud calculation platform of Beijing University of Chemical Technology (BUCT) are both greatly appreciated.

Appendix A. Supporting information

Supplementary data associated with this article can be found in the online version at http://dx.doi.org/10.1016/j.nanoen.2016.08.002.

References

[1] P. Akcora, H. Liu, S.K. Kumar, J. Moll, Y. Li, B.C. Benicewicz, L.S. Schadler, D. Acehan, A.Z. Panagiotopoulos, V. Pryamitsyn, V. Ganesan, J. Ilavsky, P. Thiyagarajan, R.H. Colby, J.F. Douglas, Nat. Mater. 8 (2009), 354-U121.
[2] T. Ramanathan, A.A. Abdala, S. Stankovich, D.A. Dikin, M. Herrera-Alonso, R. D. Piner, D.H. Adamson, H.C. Schniepp, X. Chen, R.S. Ruoff, S.T. Nguyen, I. A. Aksay, R.K. Prud'homme, L.C. Brinson, Nat. Nanotechnol. 3 (2008) 327–331.
[3] H. Oh, P.F. Green, Nat. Mater. 8 (2009) 139–143.
[4] J. Suhr, N. Koratkar, P. Keblinski, P. Ajayan, Nat. Mater. 4 (2005) 134–137.
[5] N.A. Koratkar, J. Suhr, A. Joshi, R.S. Kane, L.S. Schadler, P.M. Ajayan, S. Bartolucci, Appl. Phys. Lett. 87 (2005) 063102.
[6] A.C. Balazs, T. Emrick, T.P. Russell, Science 314 (2006) 1107–1110.
[7] N. Jouault, D. Lee, D. Zhao, S.K. Kumar, Adv. Mater. 26 (2014) 4031–4036.
[8] S. Srivastava, J.L. Schaefer, Z.C. Yang, Z.Y. Tu, L.A. Archer, Adv. Mater. 26 (2014) 201–233.
[9] J.B. Hooper, K.S. Schweizer, Macromolecules 39 (2006) 5133–5142.
[10] J. Liu, Y.G. Gao, D.P. Cao, L.Q. Zhang, Z.H. Guo, Langmuir 27 (2011) 7926–7933.
[11] L. Staniewicz, T. Vaudey, C. Degrandcourt, M. Couty, F. Gaboriaud, P. Midgley, Sci. Rep. 4 (2014) 7389.
[12] G. Heinrich, M. Kluppel, Filled Elastomers Drug Delivery Systems, 160, 2002, pp. 1–44.
[13] J. Voelcker, 1.2 Billion Vehicles On World Roads Now, 2 Billion By 2035 can be found under ⟨http://www.greencarreports.com/news/1093560_1-2-billion-vehicles-on-worlds-roads-now-2-billion-by-2035-report⟩, 2014.
[14] W.D. NRC, National Research Council of the National Academies, Transportation Research Board, Special Report, 2006.
[15] ⟨http://eur-lex.europa.eu/legal-content/EN/ALL/?uri=CELEX:32009R1222⟩.
[16] A.V. Ruzette, L. Leibler, Nat. Mater. 4 (2005) 19–31.
[17] X. Liu, S.H. Zhao, X.Y. Zhang, X.L. Li, Y. Bai, Polymer 55 (2014) 1964–1976.
[18] J. Liu, Y.L. Lu, M. Tian, F. Li, J.X. Shen, Y.Y. Gao, L.Q. Zhang, Adv. Funct. Mater. 23 (2013) 1156–1163.
[19] K. Kremer, S.T. Grest, J. Chem. Phys. 92 (1990) 5057–5086.
[20] T. Aoyagi, T. Honda, M. Doi, J. Chem. Phys. 117 (2002) 8153–8161.
[21] J. Liu, D.P. Cao, L.Q. Zhang, J. Phys. Chem. C112 (2008) 6653–6661.
[22] K. Binder, J. Baschnagel, W. Paul, Prog. Polym. Sci. 28 (2003) 115–172.
[23] M.P. Allen, D.J. Tildesley, Computer Simulation of Liquids, Oxford University Press, New York, 1987.
[24] M. Rubinstein, R.H. Colby, Polymer Physics, Oxford University Press, Oxford, UK, 2003.
[25] D.R. Rottach, J.G. Curro, J. Budzien, G.S. Grest, C. Svaneborg, R. Everaers, Macromolecules 40 (2007) 131–139.
[26] S. Plimpton, J. Comput. Phys. 117 (1995) 1–19.

Jun Liu is an associate professor of Beijing University of Chemical Technology(BUCT). He obtained his Phd at BUCT, and carried out his post-doc in University of Michigan, Ann Arbor. His research work is focused on designing and fabricating novel polymer nanocomposites through computer simulation and experimental tools.

Zijian Zheng is a Ph.D candidate at Beijing University of Chemical Technology. His expertize covers exploring the relationship between microstructure and macro-mechanics of polymer nanocomposites through Molecular Dynamics simulation. He has published several papers such as Nanotechnology, RSC advances and so on.

Fanzhu Li is a Ph.D candidate of Beijing University of Chemical Technology. His main research interests are the relationship between microstructure and properties of elastomer nanocomposites through finite element method. He has published several papers in International Journal of Fatigue, Composites Part B: Engineering and so on.

Weiwei Lei is a Ph.D candidate of Beijing University of Chemical Technology. His interests are adopting the experimental method to synthesize novel elastomer nanocomposites.

Yangyang Gao is a Ph.D candidate of Beijing University of Chemical Technology. His interests are probing the relationship between microstructure and macro-mechanics of polymer nanocomposites through Molecular Dynamics simulation. He has published several papers in Soft Matter, Physical Chemistry Chemical Physics and so on.

Youping Wu is a Professor of Beijing University of Chemical Technology. Her research directions are focused on studying the abrasion resistance, wet skid and rolling resistance of rubber tires.

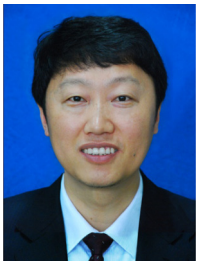

Liqun Zhang is a Professor of Beijing University of Chemical Technology. His research interests focus on rubber science and technology, polymer nanocomposites, bio-based polymeric materials and so on. He has received various famous awards such as National Outstanding Youth Foundation, Changjiang Scholar Professor of Ministry of Education of China, Sparks-Thomas sci-tech award of Rubber Division of American Chemical Society, Science of Chemical Engineering of Japan (SCEJ) Research award, Morand Lambla Award of International Polymer Processing Society. He has published over 300 peer-reviewed papers, (co-)authors of 8 books (chapters) and has given over 60 plenary/keynote/invited lectures in international conferences.

Zhong Lin Wang is the Hightower Chair in Materials Science and Engineering, Regents' Professor, Engineering Distinguished Professor at Georgia Tech. Dr. Wang is a foreign member of the Chinese Academy of Sciences, fellow of American Physical Society, fellow of AAAS, fellow of Microscopy Society of America, and fellow of Materials Research Society. He has been awarded the MRS Medal and Burton Medal. He has made original contributions to the fundamental physics and applications of oxide nanobelts and nanowires. His discovery in nanogenerators establishes the principle and technological roadmap for harvesting mechanical energy from environment and biological systems.